View metadata, citation and similar papers at core.ac.uk

brought to you by CORE

provided by University of Dundee Online Publications

University of Dundee

An Experimental Study of the Embedment of a Dynamically Installed Anchor in Sand

Chow, S. H.; O'Loughlin, Conleth D. ; Gaudin, Christophe ; Knappett, Jonathan A.; Brown, Michael J.; Lieng, Jon T.

Published in:
Offshore Site Investigation and Geotechnics: Smarter Solutions for Future Offshore Developments

DOI:
10.3723/OSIG17.1019

Publication date:
2017

Document Version
Peer reviewed version

Link to publication in Discovery Research Portal

Citation for published version (APA):
Chow, S. H., O'Loughlin, C. D., Gaudin, C., Knappett, J. A., Brown, M. J., & Lieng, J. T. (2017). An Experimental Study of the Embedment of a Dynamically Installed Anchor in Sand. In *Offshore Site Investigation and Geotechnics: Smarter Solutions for Future Offshore Developments: Proceedings of the 8th International Conference, held 12–14 September 2017 at the Royal Geographical Society, London* (Vol. 1-2, pp. 1019-1025). Society for Underwater Technology. https://doi.org/10.3723/OSIG17.1019

General rights
Copyright and moral rights for the publications made accessible in Discovery Research Portal are retained by the authors and/or other copyright owners and it is a condition of accessing publications that users recognise and abide by the legal requirements associated with these rights.

- Users may download and print one copy of any publication from Discovery Research Portal for the purpose of private study or research.
- You may not further distribute the material or use it for any profit-making activity or commercial gain.
- You may freely distribute the URL identifying the publication in the public portal.

Take down policy
If you believe that this document breaches copyright please contact us providing details, and we will remove access to the work immediately and investigate your claim.

Download date: 17. Aug. 2021

AN EXPERIMENTAL STUDY OF THE EMBEDMENT OF A DYNAMICALLY INSTALLED ANCHOR IN SAND

SH Chow, CD O'Loughlin and C Gaudin
Centre for Offshore Foundation Systems, Perth, Australia
JA Knappett and MJ Brown
Civil Engineering, University of Dundee, Dundee, UK
JT Lieng
GeoProbing Technology, Norway

Abstract
This paper presents a novel dynamically installed anchor concept suitable for sand. The anchor, referred to as the DPAIII, uses a thin 'blade-like' design to reduce bearing resistance during penetration, and comprises a lower plate attached to an upper removable follower. The anchor is installed through the kinetic energy it gains during free-fall in water. After embedment, the upper follower is removed leaving the lower plate anchor vertically embedded in the sand. This paper examines the embedment potential of the DPAIII through centrifuge tests conducted at 100*g* in both loose and dense sand, using a model DPA III with different follower masses, impacting the model sand bed at two different velocities. The centrifuge tests show promising results, with anchor tip embedment in the range of 0.9 to 2.2 times the lower plate length. The tip embedment is found to be a function of the soil relative density, anchor mass and impact velocity.

1. Introduction

Anchoring in a sandy seabed is constrained by difficulties in anchor installation, particularly to achieve the required embedment in dense sand. Existing anchoring solutions for sand, such as piles and drag embedded plate anchors, typically involve lengthy installations, and in the case of drag embedment anchors, uncertainty over final penetration depth and thus holding capacity. This has the potential to seriously impact the economics of emerging marine renewable energy technologies, which may be deployed in complex arrays requiring large numbers of accurately positioned anchors. Many of the proposed early array sites have sandy seabeds or sand layers of limited depth over rock and it is thus imperative to develop new robust technologies to reduce total installation times and hence costs.

A possible solution requiring shorter installation time are dynamically installed anchors, which are allowed to free-fall from vessels and embed into the seabed by their kinetic energy. Some examples of dynamic anchors including torpedo anchors (Medeiros, 2002), Deep Penetrating Anchors (Lieng et al., 2000), dynamically embedded plate anchors (O'Loughlin et al., 2014) and the OMNI-Max anchor (Shelton, 2007) have been developed for the offshore oil and gas industry. The feasibility and performance of these anchors has been demonstrated for clay. They are however, generally perceived to be less suitable for sand due to their potential limited embedment in granular soils. For instance, centrifuge tests on deep penetrating anchors (DPAs) have revealed that DPA tip embedment in silica flour is about one-third of the anchor length, compared with over two times the anchor length in normally-consolidated kaolin clay at similar impact velocities (Richardson, 2008). However, alternative dynamically installed anchor designs may achieve higher penetrations in sand, and prove to be a viable anchoring solution for granular seabed deposits.

One of the main aims of the EU-funded project, GeoWAVE (www.geowave-r4sme.eu), is to develop such anchoring concepts initially based around mooring wave energy converters, but which will also be applicable to many other technologies requiring cost-effective mooring in sand. Examples include floating offshore wind turbines, aquaculture farms and other marine renewable energy devices along with the potential for scaled up application to oil and gas developments.

This paper introduces a new dynamically installed anchor concept, referred to as the DPAIII, and reports data from centrifuge tests undertaken to quantify the embedment potential in loose and dense saturated sand.

2. Design Concept of DPAIII

The design and installation concept of the DPAIII anchor are illustrated in Figure 1. The anchor adopts a thin 'blade-like' design which increases penetration potential in sand compared with existing dynamically installed anchor designs that typically utilise solid cylindrical shafts with conical or ellipsoidal tips (O'Loughlin et al., 2004). The DPAIII anchor features a plate at the lower end attached to an upper removable follower and takes the form of two thin blades projecting from a central core. The thin blades on the lower plate anchor are tapered to maximise embedment potential. Two additional fins are added to the top of the upper follower (Figure 1) to improve hydrodynamic stability during freefall in water. The DPAIII is installed in a similar manner to previous types of dynamically installed anchors, and utilises the upper removable follower to provide the necessary additional mass to achieve the required anchor embedment. Following embedment, the follower is retrieved to the installation vessel for re-use in the next installation, leaving the plate anchor vertically embedded in the seabed.

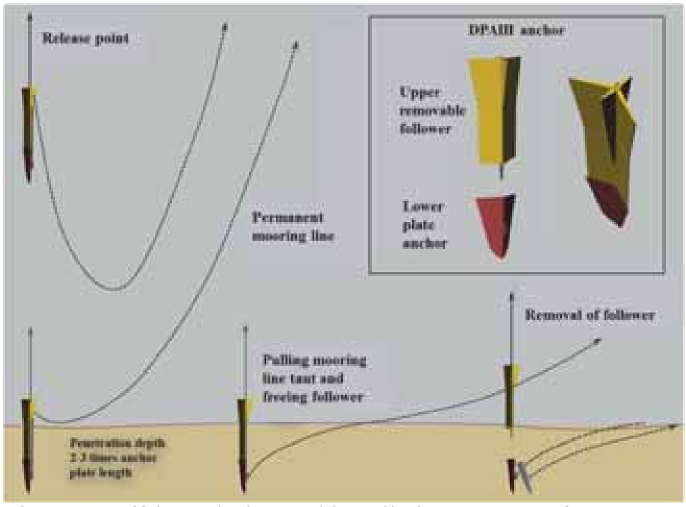

Figure 1: Offshore design and installation concept of DPAIII anchor

3. Centrifuge Tests

3.1 Model DPAIII anchor

Figure 2 shows the 1:100 reduced scale model DPAIII anchor used in the centrifuge tests. The model follower does not feature the two additional stabilizing fins as, in the centrifuge tests, the anchor is installed using an installation guide (see Section 3.3) and the follower is not expected to embed fully in the sand. Similar to the prototype anchor, the model anchor takes the form of two thin blades projecting from a central core, with blade thickness, $t = 0.76$ mm from the core thinning out to $t = 0.1$ mm at the edge. The lower plate anchor with mass, $m_p = 1.28$ g and length, $L_p = 24$ mm, features a padeye, which is located at an eccentricity, $e_n = 2.1$ mm from the centre of the core and $e_p = 13$ mm from the top of the plate respectively (see Figure 3). Three simplified followers with different lengths, $L_f = 46$, 65 and 84 mm, were fabricated to investigate the effect of overall anchor mass on anchor embedment. The three different lengths of followers produce overall anchor masses, $m = 5.55$, 7.28 and 8.88 g and corresponding follower mass to plate anchor mass ratios, m_f/m_p = 3.3, 4.7 and 5.9. Although these overall dimensions and masses imply that a full scale prototype anchor would have an assembled overall length, L of up to 10.8 m and an overall maximum dry mass of 8.8 tonne, the anchor size will be highly dependent upon the required mooring line loads and the geotechnical behaviour of the embedded plate (which has yet to be established). If required, the anchor can be scaled up, increasing the overall mass, and the geometry optimised to provide greater penetration potential.

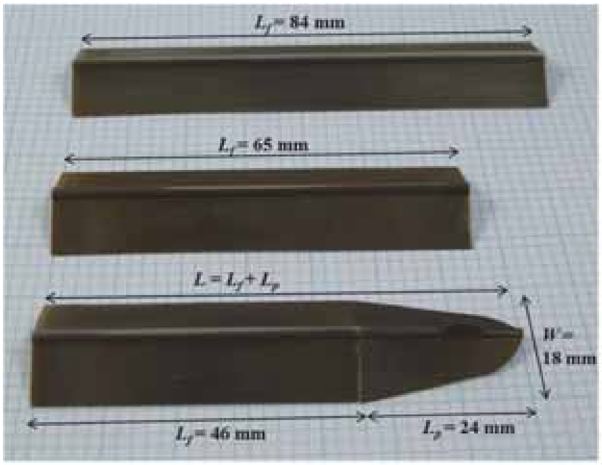

Figure 2: 1:100 reduced scale model DPAIII anchor

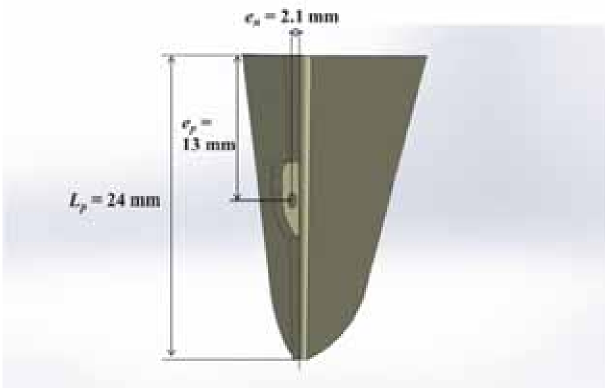

Figure 3: Schematic showing the geometrical details of the model plate anchor

3.2 Soil properties and preparation technique

The sand used in the centrifuge study is a commercially available silica sand with properties as listed in *Table 1*. The sand samples used in the centrifuge tests were prepared by air pluviation using a sand rainer with automated speed control, adjustable drop height and hopper opening width, allowing accurate control of the sand bed density.

The sand was rained into a centrifuge strong box with internal dimensions 650 × 390 × 325mm (length × width × depth) such that the final sample dry density was either 1521 or 1702kg/m^3 (corresponding to loose and dense conditions with relative densities D_r = 23% and 80% respectively). The surface of the sand was then vacuumed level to produce a final sample height of 225mm. The sample was saturated by 'drip-feeding' water over a geotextile fabric placed on top of the sample. About 40mm of free water was maintained above the sand surface during the centrifuge testing.

Table 1: Properties of UWA superfine silica sand

Specific gravity, G_s	2.65
Particle size, d_{10}, d_{50}, d_{60}	0.10, 0.19, 0.22 mm
Minimum dry density, ρ_{min}	1460 kg/m^3
Maximum dry density, ρ_{max}	1774 kg/m^3
Critical state friction angle, ϕ'_{cs}	30° (Lehane & Liu 2013)

3.3 Centrifuge test programme and procedure

The centrifuge tests were performed at an acceleration of 100 *g* using the UWA beam centrifuge (Randolph et al., 1991). Fourteen free-fall DPAIII tests were conducted as listed in *Table 2* considering the following variables:

- sand relative density, D_r (23, 80%);
- anchor mass ratio, m_f/m_p (3.3, 4.7, 5.9); and
- impact velocity, v_i (~5, ~18 m/s).

As described below, the two different impact velocities were achieved by adjusting the anchor release height in the centrifuge, in the same way as different impact velocities would be obtained in the prototype case by releasing the anchor in the water column from different heights above the seabed. Although the terminal velocity of the DPA III has not been established, a terminal velocity of 18 m/s would be expected assuming a drag coefficient, C_d = 0.02 (Shelton, 2007). In addition to the DPAIII tests, cone penetrometer tests were performed at a constant penetration rate of 1mm/s to assess strength variations between samples.

The experimental arrangement is shown in Figure 4. Dynamic installation of the DPAIII in the centrifuge was identical to that described in detail by O'Loughlin et al. (2004) for installation of dynamically installed anchors, and as such only a brief description is provided here. The DPAIII was installed by allowing the anchor to free-fall through the elevated acceleration field in the centrifuge through an installation guide. This guide, which was necessary to prevent lateral movement of the anchor during free-fall due to Coriolis acceleration, comprised of a rectangular stainless steel block with internal cuts to accommodate the two thin blades of the DPAIII model anchor. The anchor was located in the guide at a preselected release height (depending on the target impact velocity) using a release cord attached to the top of the follower. Anchor release was achieved in-flight using a resistor which, when powered, heated and subsequently burned through the release cord, triggering the drop. At the end of the penetration, the final embedment depth of the anchor was measured using a steel ruler.

Taking into consideration the radial acceleration field in the centrifuge, the DPAIII free-fall tests were restricted to the centre line of the strong box. In order to minimise potential interaction and boundary effects, a spacing of 75mm (equivalent to ~ 20D_e, where D_e is the equivalent anchor diameter) was permitted between adjacent tests and a spacing of 100mm (~ 25D_e) was permitted between the installation sites and the rigid walls of the strongbox.

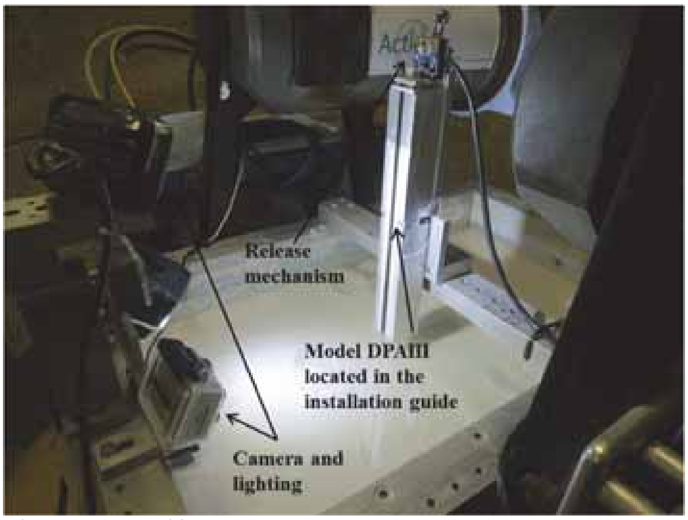

Figure 4: Centrifuge DPAIII test setup

Table 2: Test programme and summary of test results (at prototype scale)

Test details		Anchor overall mass, *m* (kg)	Anchor mass ratio, m_f/m_p	Impact velocity, v_i (m/s)	Final embedment depth, *H** (m)
Sample 1 (loose)	1	8880	5.9	18.2	5.27
	2	8880	5.9	18.1	5.28
	3	8880	5.9	5.2	2.55
	4	7280	4.7	18.2	4.73
	5	7280	4.7	5.2	2.05
	6	5550	3.3	18.2	4.13
	7	5550	3.3	5.8	2.13
Sample 2 (dense)	8	8880	5.9	18.1	3.70
	9	8880	5.9	18.1	3.80
	10	8880	5.9	4.9	2.05
	11	7280	4.7	18.1	3.40
	12	7280	4.7	18.1	3.30
	13	5550	3.3	18.1	3.05
	14	5550	3.3	18.1	2.95

* Measured to the tip of the plate anchor

As the plate anchor thickness (*t* = 0.76 to 0.1mm) brackets the mean grain size (d_{50} = 0.19mm), the anchor installation resistance may be affected by grain size effects. This aspect of the modelling problem is being considered in a parallel study and will be reported elsewhere. The grain size effect will potentially reduce anchor penetration in the centrifuge tests, but will not affect the dependence of anchor mass ratio, impact velocity and relative density on anchor embedment (as any grain size effect experienced will be relative), which is the main focus of this experimental programme.

4. Test Results

4.1 Sample characterisation

At least two cone penetrometer tests were performed at a penetration rate of 1 mm/s in each sample using a 10 mm diameter model cone penetrometer. The cone tip resistance, q_c, is plotted against prototype depth in Figure 5. The tip resistance increases with depth in both samples, which reflects the increase in vertical effective stress with depth. The higher tip resistance profiles for Sample 2 also reflects the higher sand density compared with Sample 1 (D_r = 23% and 80% for Sample 1 and 2 respectively).

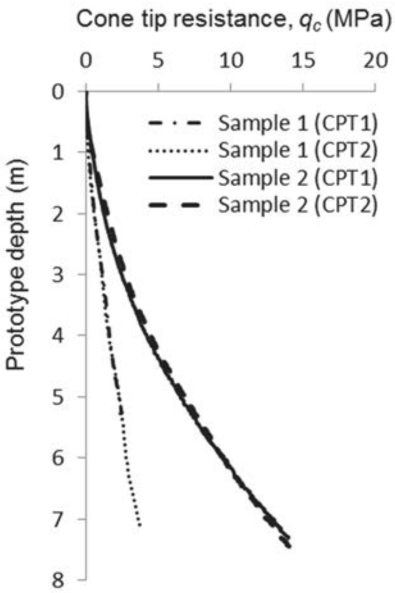

Figure 5: Cone tip penetration resistance profiles

4.2 Impact velocity and embedment depth

The test results are summarised in *Table 2*, which lists the impact velocities and the final plate anchor tip embedment depths of all free-fall DPAIII tests. Previous centrifuge studies on dynamically installed anchors used photo emitter/receivers to measure the anchor velocity as it travelled along the installation guide (e.g. O'Loughlin et al., 2004, 2009), and by extrapolation at the soil surface. However as the very thin plate thickness of the DPAIII model anchor prevented such measurements, anchor impact velocity was estimated by considering the theoretical evolution of anchor velocity as it travels radially through the increasing acceleration field in the centrifuge by considering the change in anchor velocity over a small radius increment (Richardson, 2008), during which the acceleration is assumed to remain constant and formulated as:

$$v_{i+1} = \sqrt{v^2 + 2a\Delta r} \quad (1)$$

where v_{i+1} is the anchor velocity at the end of the increment, v_i is the anchor velocity at the beginning of the increment, a is the gravitational acceleration equal to ωr^2, ω is the rotational velocity of the centrifuge, r is the radius from the rotational axis of the centrifuge and Δr is the radius increment being considered. The theoretical impact velocity is known to be affected by the interface friction developed between the anchor and the installation guide (O'Loughlin et al., 2004; Gaudin et al., 2013). Hence the estimated v_i was reduced by a factor of 0.925, as established during previous centrifuge studies on dynamically installed penetrometers (Chow et al., 2014).

The test results in *Table 2* show good test repeatability with identical final embedment depth measurements from two repeat tests (e.g. Tests 1 and 2). The relative influence of the three variables (D_r, m_f/m_p and v_i) on the anchor final embedment depths is discussed in the following sections.

4.3 Effect of relative density

The effect of relative density, D_r is examined for tests involving impact velocity, v_i of ~18m/s. As shown in Figure 6, deeper embedment is achieved in the looser sand. Depending on the anchor mass ratio, embedment ratios H/L_p of 1.72 to 2.20 are achieved for Sample 1 (D_r = 23%) compared with H/L_p of 1.25 to 1.56 for Sample 2 (D_r = 80%). This corresponds to approximately 40% higher embedment in the loose sand sample. The higher embedment in loose sand is considered to be due to the lower penetration resistance (as reflected in the q_c profiles on Figure 5), but also to a higher potential to accommodate volume changes during shearing, with less work required (and hence less energy dissipated) to displace soil during penetration.

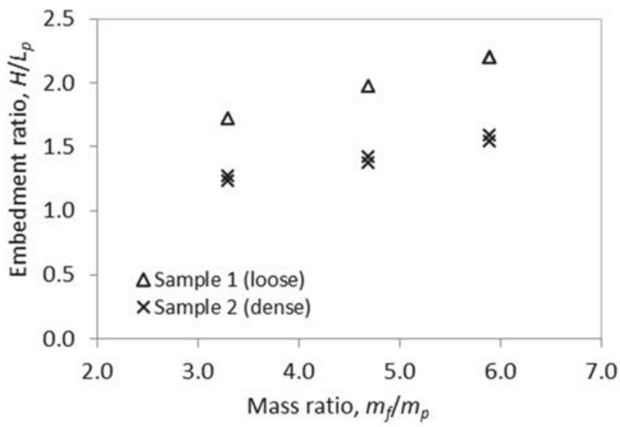

Figure 6: Higher anchor tip embedment with reducing density and increasing mass ratio (all tests conducted at v_i ~18m/s)

4.4 Effect of anchor mass ratio

The effect of anchor mass ratio, m_f/m_p, on anchor embedment is illustrated in Figure 6 and Figure 7. The embedment ratio H/L_p, is found to increase linearly with increasing mass ratio, m_f/m_p. The rate of increase in embedment ratio with mass ratio, appears to be independent of relative density (Figure 6), but is higher for higher impact velocities (Figure 7). In general, an average increase of 27% in embedment ratio is observed for a corresponding increase in mass ratio from 3.3 to 5.9.

4.5 Effect of impact velocity

The effect of two impact velocities (v_i ~5 and ~18 m/s) on the anchor embedment is investigated in Sample 1 as shown in Figure 7. For the same mass ratio, anchor embedment ratios H/L_p of 1.72 to 2.20 are achieved at impact velocity v_i ~18 m/s, compared with H/L_p = 0.85 to 1.06 at lower impact velocity v_i ~5 m/s. Overall, a two-fold increase in embedment ratio can be achieved by increasing the impact velocity v_i from ~5 to ~18 m/s in loose sand.

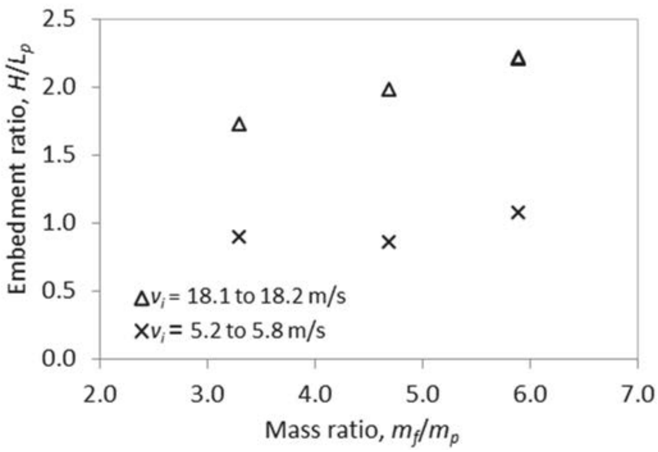

Figure 7: Higher anchor tip embedment with increasing aspect ratio and impact velocity (all tests conducted in loose sand)

5. Discussion

The DPAIII anchor has achieved embedment ratios, H/L_p in the range 0.85 to 2.2, depending on the sand density, mass ratio and impact velocity. Equivalent prototype anchor embedment may be higher if grain size effects have influenced the embedment achieved in the centrifuge tests. The DPAIII embedment achieved in this study are compared with existing DPA centrifuge test data reported by Richardson (2008) in dense silica flour, medium dense calcareous sand and normally consolidated clay as shown in Figure 8a. Compared to the thin-bladed DPAIII, the DPA of length L, consists of a solid cylindrical shank with ellipsoidal or hemispherical tips (as shown in Figure 8a).

The DPAIII has achieved higher final embedment depths than the DPA in silica flour (d_{50} of 45 μm), the latter requiring a much higher prototype mass, m = 118.4 tonnes and impact velocity, v_i = 28.7 m/s (Richardson, 2008). However, deeper embedment was achieved by the DPA in the crushable calcareous sand and the normally consolidated kaolin clay. In general, similar dependency on anchor mass and impact velocity is observed in the DPA test data for both clay and sand.

However, a more meaningful comparison can be made by normalising the embedment depth by the anchor length, L or L_p, as this is a better reflection of the subsequent anchor capacity. Figure 8b shows this comparison, where the normalised embedment data are plotted against the kinetic energy of the anchor at the mudline, which permits comparisons of test data with different masses and impact velocities. Figure 8b clearly demonstrates that the DPAIII achieves similar normalised embedment in sand to the DPA in normally consolidated clay, and higher embedment than the DPA in medium dense calcareous sand and dense silica flour. This illustrates the benefit of the DPAIII design, which is able to penetrate sufficiently to achieve the required capacity with its thin-blade geometry and a sufficiently heavy removable/reusable follower. To the authors' knowledge, this is the first demonstration of the possibility of using dynamically embedded anchors in siliceous sand.

Considering the promising embedment potential of the DPAIII, it is of interest to investigate its pull-out capacity. Results from preliminary centrifuge pull-out tests in dense sand suggest that the monotonic anchor capacity for the equivalent prototype anchor is around 433 kN for an embedment ratio, H/L_p = 2 and a zero degree mudline loading angle (i.e. a catenary mooring arrangement), which corresponds to an anchor capacity factor, N_γ = 3.5. This capacity is based on the anchor geometry and scale considered in this paper. Higher capacities may be realised by increasing the anchor scale, and also by considering the anchor geometry, particularly the eccentricity of the anchor padeye.

6. Conclusions

A new dynamically installed anchor, termed the DPAIII, is being developed for application in sandy seabeds. The embedment potential of the anchor, which features a thin blade-like design and a removable follower, has been investigated through centrifuge tests performed at 100*g*. The centrifuge tests were conducted in both loose and dense saturated silica sand samples, and considered anchor mass ratios, m_f/m_p = 3.3, 4.7 and 5.9, and anchor impact velocities, v_i = 5 and 18 m/s. The anchor was found to embed between 0.9 and 2.2 times the lower plate (anchor) length. The anchor final embedment depth is found to increase with decreasing relative density and increasing mass ratio and impact velocity. The centrifuge tests reported here have demonstrated the embedment potential of a dynamically installed anchor in sand. Further centrifuge tests and numerical simulation, aiming at quantifying and modelling anchor capacity under monotonic and cyclic loading are ongoing and will be reported in due course.

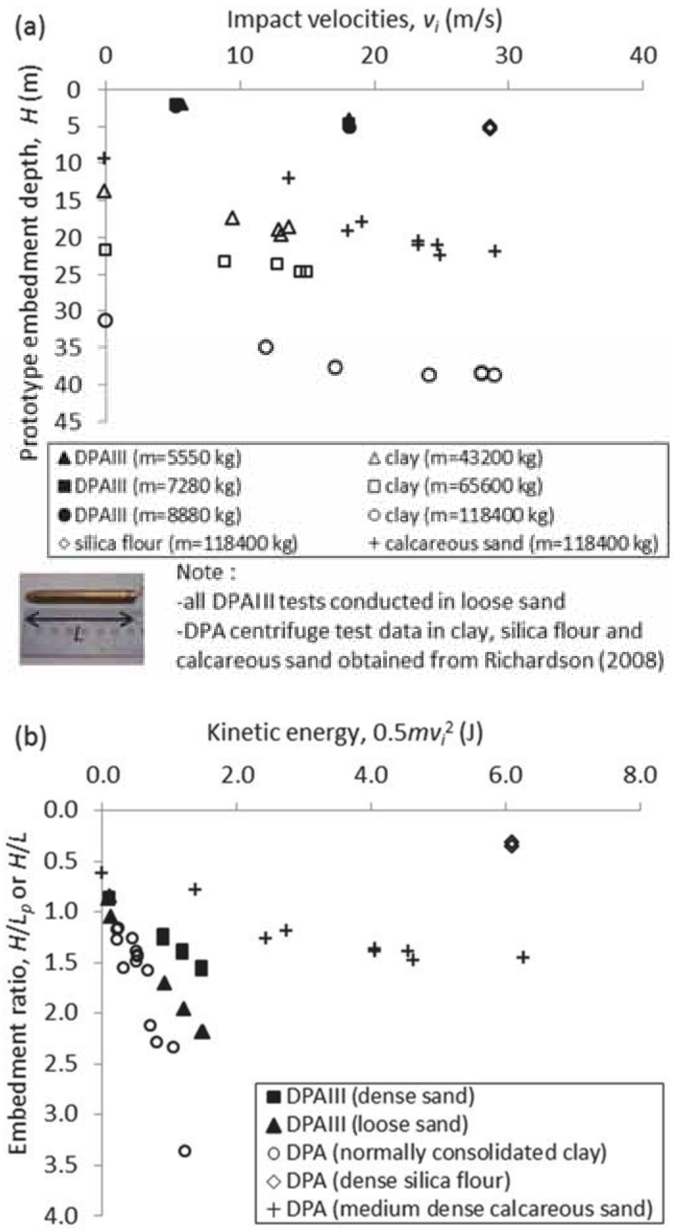

Figure 8: Comparison between DPAIII and DPA: (a) similar dependency on mass and impact velocities; (b) better penetrability of the DPAIII than the DPA in sand

7. Acknowledgements

This work forms part of the activities of the Centre for Offshore Foundation Systems (COFS), currently supported as a node of the Australian Research Council Centre of Excellence for Geotechnical Science and Engineering. The research leading to these results has received funding from the European Union Seventh Framework Programme (FP7/2007-2013) under grant agreement n° 287056.

8. References

Chow SH, O'Loughlin CD and Randolph MF. (2014). Soil strength estimation and pore pressure dissipation for free-fall piezocones in clay. *Geotechnique* 64(10): 817-827.

Gaudin C, O'Loughlin CD, Hossain MS and Zimmerman EH. (2013). The performance of dynamically embedded anchors in calcareous silt. *Proc. 32nd Int. Conf. on Ocean, Offshore and Arctic Engineering*, Nantes, France: pp. V006T10A006.

Lehane BM and Liu QB. (2013). Measurement of shearing resistance characteristics of granular materials at low stress levels in a shear box. *Geotech Geol Eng* 31: 329-336.

Lieng JT, Kavli A, Hove F and Tjelta TI. (2000). Deep penetrating anchor: further development, optimization and capacity verification. *Proc. 10th Intern. Offshore and Polar Engineering Conference, Seattle, Washington:* 410–416.

Medeiros Jr CJ. (2002). Low cost anchor system for flexible risers in deep waters. *Proc. Offshore Technology Conference*, Houston: p. 14151.

O'Loughlin CD, Randolph MF and Richardson MD. (2004). Experimtental and Theoretical Studies of Deep Penetrating Anchors. *Proc. Offshore Technology Conference*, Houston: p. 16841.

O'Loughlin CD, Richardson MD and Randolph MF. (2009). Centrifuge tests on dynamically installed anchors. *Proc. 28th Int. Conf. on Ocean, Offshore and Arctic Engineering*, Honolulu, Hawaii: 391-399.

O'Loughlin CD, Blake AP, Richardson MD, Randolph MD and Gaudin C. (2014). Installation and capacity of dynamically installed plate anchors as assessed through centrifuge tests. *Ocean Engineering* 88: 204-213.

Randolph MF, Jewell RJ, Stone KJL and Brown TA. (1991). Establishing a new centrifuge facility. *Proc. Int. Conf. Centrifuge 91, Boulder*: 3–9.

Richardson MD. (2008). *Dynamically installed anchors for floating offshore structures*. PhD thesis, The University of Western Australia.

Shelton JT. (2007). OMNI-Maxtrade Anchor Development and Technology. *Proc. OCEANS Conference, Vancouver*, IEEE: 1-10.

Notation

a gravitational acceleration

C_d	drag coefficient
d_{10}, d_{50}, d_{60}	sand particle size at 10%, 50% and 60% passing
DPA	Deep Penetrating Anchor
D_e	equivalent anchor diameter
D_r	relative density
e_n	padeye eccentricity normal to anchor
e_p	padeye eccentricity parallel to the anchor
Gs	specific gravity
H	final embedment depth
H/L_p	tip embedment ratio
t	blade thickness
L	overall anchor length
L_f, L_p	follower length, lower plate anchor length
m	overall anchor mass
m_f, m_p	follower mass, lower plate anchor mass
N_γ	anchor capacity factor
q_c	cone tip penetration resistance
r	radius from the rotational axis of the centrifuge
v_i	impact velocity
ϕ'_{cs}	critical state friction angle
ρ_{min}, ρ_{max}	minimum and maximum dry density